



PERGAMON

Solid State Communications 112 (1999) 371–374

solid
state
communications

www.elsevier.com/locate/ssc

Negative differential resistance and the transition to current self-oscillation in GaAs/AlAs superlattices

J.N. Wang^{a,*}, B.Q. Sun^{a,b}, X.R. Wang^a, H.L. Wang^b

^aPhysics Department, The Hong Kong University of Science and Technology, Clear Water Bay, Hong Kong, SAR, China

^bNLSM, Institute of Semiconductors, Chinese Academy of Sciences 100083, Beijing, China

Received 8 July 1999; accepted 5 August 1999 by P. Sheng

Abstract

We investigate the transition from static to dynamic electric field domains (EFDs) in a doped GaAs/AlAs superlattice (SL). We show that a transverse magnetic field and/or the temperature can induce current self-oscillations. This observation can be attributed to the negative differential resistance (NDR) effect. Transverse magnetic field and the temperature can increase the NDR of a doped SL. A large NDR can lead to an unstable EFD in a certain range of d.c. bias. © 1999 Elsevier Science Ltd. All rights reserved.

Keywords: A. Semiconductors; D. Tunneling

There has been a long lasting interest [1–26] in the vertical electron transport of superlattices (SLs) since the pioneering work of Esaki and Chang [1,2] on the electric field domain (EFD) formation in doped SLs. Many interesting phenomena related to the negative differential resistance (NDR) have been found in SLs, including sawtooth-like current–voltage, $I(U)$, characteristic on the sequential resonance tunneling plateau [14–19], current self-oscillations [20–24] and chaos [25]. Self-oscillation has been observed in both doped and undoped SL systems [18–23]. So far, previous studies of current self-oscillation in SLs have been focused on the effect of changing the carrier concentration through either the continuous illumination of a laser light [24] or doping [20,21]. It is understood that the sawtooth-like branch of the current–voltage characteristic is related to the formation of stationary EFD while the current self-oscillations are attributed to the traveling of the domain boundary [9–13]. The carrier density effects can be explained by solving a set of coupled partial differential equations [9–13]. Under a d.c. bias within a certain range of carrier concentration, this set of equations has solutions of the temporal current self-oscillations. Solutions of current self-oscillations disappear outside this carrier

concentration range. However, the theory gives no simple criterion for the current self-oscillations. Neither does it provide a scenario of how external fields, like the magnetic field and/or the sample temperature, affect the transition from sawtooth-like current–voltage characteristic to current self-oscillations.

In this paper, we show, for the first time to our knowledge, that a transverse magnetic field and the sample temperature can also control the transition from stable to unstable EFD formation. In contrast to previous studies, in the present work we show the NDR to be the essential element of the underlying physics [26]. This insight both unifies and generalizes the explanation for EFD stability/instability. Varying the transverse magnetic field or the temperature, changes the NDR and produces the transition from stable to unstable EFD formation.

The doped GaAs/AlAs SL studied in this work was grown by molecular beam epitaxy. The SL consists of 40 14-nm GaAs wells confined by 41 4-nm AlAs barriers. The SL is sandwiched between two n^+ GaAs layers. The central 10 nm of each GaAs well was doped with Si ($n = 2 \times 10^{17} \text{ cm}^{-3}$). The sample was fabricated into $0.1 \times 0.1 \text{ mm}^2$ mesas. We measured the $I(U)$ characteristic of the sample in a magnetic field up to 14 T perpendicular to the current direction, and at zero field at temperatures from 1.6 to 200 K, using a HP4155A semiconductor parameter

* Corresponding author.

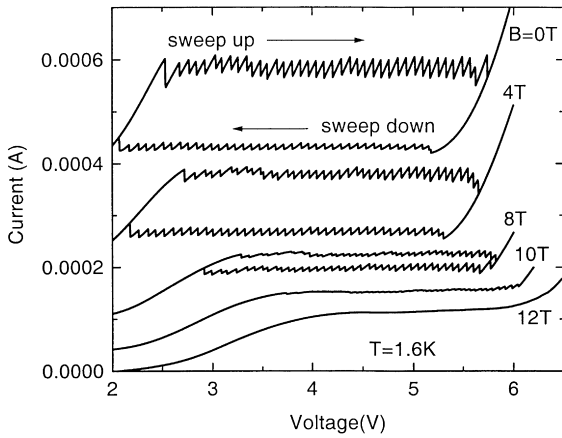


Fig. 1. The measured $I(U)$ curves at different transverse magnetic fields ($B = 0, 4, 8, 10$ and 12 T) indicated with the bias applied in both sweep-up and sweep-down directions at 1.6 K. Curves are offset for clarity.

analyzer. The current self-oscillations were recorded by a HP54600A digital oscilloscope.

We focus on the second plateau of the $I(U)$ characteristic of our sample. It is well known that the EFD forms on the plateau [1,2,9–13]. At low-field domains, electrons tunnel from the ground state in one well to the first excited state in the next while electron tunneling is from the ground state to the second excited state at high-field domains. Fig. 1 shows the measured $I(U)$ of the sample at temperature $T = 1.6$ K for different transverse magnetic fields (B) as the applied bias is swept up or down. A large hysteresis in $I(U)$ is observed at $B = 0$ T and $T = 1.6$ K, the current plateau being higher in sweep-up than in sweep-down. In both sweep directions the $I(U)$ characteristic exhibits a series

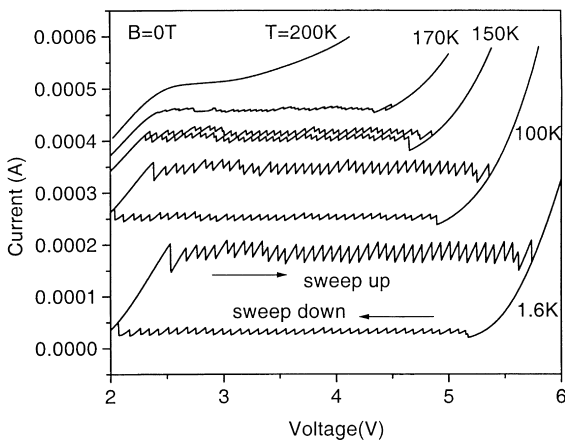


Fig. 2. The measured $I(U)$ curves in the absence of the magnetic fields for $T = 1.6, 100, 150, 170$ and 200 K with the bias applied in both sweep-up and sweep-down directions. Curves are offset for clarity.

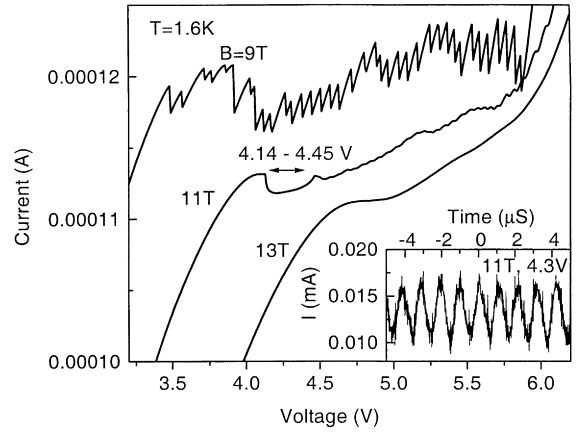


Fig. 3. Enlargement of $I(U)$ curves at $T = 1.6$ K for $B = 9, 11$ and 13 T with the bias applied in sweep-up direction. Curves are offset for clarity. The inset shows the measured temporal current oscillation at 11 T and 4.3 V.

of 40 sawtooth-like current branches, corresponding to static EFD formation. When the current jumps from one branch to the next, the charge layer at the domain boundary moves from one well to the adjacent well. Note that the number of branches observed in the experiment is as the same as the number of SL periods.

The temperature effects on the EFD formation are shown in Fig. 2. Similar results as those in Fig. 1 are obtained with $B = 0$ T when T is varied. As can be seen in Figs. 1 and 2, the hysteresis effect disappears, and the amplitude of the sawtooth oscillation in the $I(U)$ characteristic becomes very small when B is above 10 T (at $T = 1.6$ K) or when T is above 170 K (at $B = 0$ T). At these values of B and T , in

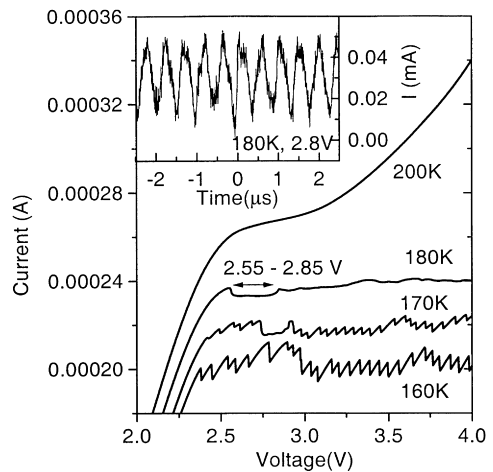


Fig. 4. Enlargement of $I(U)$ curves at $B = 0$ T for $T = 160, 170, 180$ and 200 K with the bias applied in sweep-up direction. Curves are offset for clarity. The inset shows the measured current oscillation at 180 K and 2.8 V.

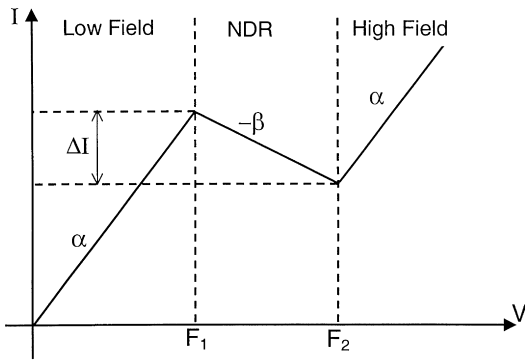


Fig. 5. Piecewise linear $I(V)$ curve where V is the bias across a single barrier. Low field region and high field region have the same slope α . NDR region has the negative differential resistance, $-1/\beta$.

a certain range of d.c. bias, temporal current self-oscillation occurs, indicating dynamic EFD formation. If the magnetic field is increased above 12.5 T, or the temperature is increased above 190 K, $I(U)$ becomes monotonic, corresponding to uniform electric field distribution. Figs. 3 and 4 are the enlargements of $I(U)$ to illustrate the transitions from sawtooth-like current-voltage characteristic to current self-oscillation, and then to uniform electric field distribution. The voltage ranges within which the current self-oscillations are observed are indicated in the figures. The insets in Figs. 3 and 4 show the current self-oscillations at $B = 11$ T, $T = 1.6$ K, d.c. bias 4.3 V and $B = 0$ T, $T = 180$ K, d.c. bias 2.8 V, respectively.

It is difficult to explain these observations based on the existing theories [9–13]. Although the observation of both stable and unstable domain formations is not new, the transition between them induced by a transverse magnetic field and a sample temperature is a new discovery. Further, these effects cannot be trivially understood from the existing theories. There would be no clear physical picture even if one could describe some of the features observed in our experiments following a well-accepted theory in the field [9–13]. On the other hand, these results can be understood in terms of the general analysis of instabilities and oscillations of the sequential tunneling current in SL given by Wang et al. [26]. They have derived general conditions for the stability of the current through a SL in which the $I(V)$ characteristic of each tunneling barrier (V being the bias across a single barrier) has a region of NDR. They show that as long as the absolute magnitude of the NDR of one barrier does not exceed the sum of the positive differential resistance (PDR) of the remaining barriers, stable domains can form. If this condition is not met, the domains are unstable and current self-oscillation occurs. While the results of Ref. [26] are general, they are very easily made quantitative by considering a highly idealized model of a SL with $N - 1$ wells separated by N barriers. We assume that the tunneling current of each barrier between any two

neighboring wells is given by the same piecewise $I(V)$ characteristic, shown in Fig. 5.

The three regions of the characteristic have slopes α , $-\beta$ and α , respectively. ΔI is the peak to valley current difference. F_1 and F_2 are the biases at the two break points indicated in Fig. 5. Stable domain formations correspond to k barriers being in the high field region (domain) and $N - k$ in the low field, where $1 \leq k \leq N$. Wang et al. show that domains are stable so long as $0 < 1/\beta < (N - 1)/\alpha$. If N is large, as in our case, unstable domains (current self-oscillation) can occur only if β is very small so that $1/\beta > (N - 1)/\alpha$. As β is decreased by some external influence the system switches from the stable EFD formation to the unstable.

The model also accounts for the general shape of the SL's $I(U)$ characteristic in the regime of stable domain formation. When the external bias, U , is swept up, we start with all barriers in the low field region so that the bias across each barrier is $V = U/N$. The current increases with increasing U and reaches a maximum value of $I = \alpha F_1$ when $U = NF_1$. A small increase of U moves one barrier into the high field region, so that the bias across the remaining low field barriers must decrease to compensate. The current then jumps to a lower value. Further increase of U increases I , until V across the low field barriers reaches F_1 and $I = \alpha F_1$ again. A further small increase of U moves another barrier into the high field region. As U increases, the process repeats until all the barriers are in the high field region. Thus the $I(U)$ characteristic of the SL exhibits the well-known sawtooth form with N branches. When the bias is swept down, on the other hand, we start with all barriers in the high field region. As U decreases, the current in the sawtooth region reaches a minimum value of $I = \alpha F_1 - \Delta I$, where $\Delta I = \beta(F_2 - F_1)$, when $U = NF_2$. A small decrease of U moves one barrier into the low field region, so that the bias across the remaining high field barriers increases to compensate. The current then jumps to a higher value. Thus the model explains the observed current hysteresis effect (see Figs. 1 and 2). The hysteresis defined as the difference between the maximum current in sweep up and minimum current in sweep down, in the sawtooth region of $I(U)$ is, ideally, equal to ΔI .

The model also predicts the peak to valley difference δI of the sawtooth oscillation in the current. We find $\delta I = \Delta I(1 + \alpha/\beta)/N$. As β decreases, δI approaches ΔI , and when $\delta I = \Delta I$ (so that there is no hysteresis) the condition for instability (given above as $1/\beta > (N - 1)/\alpha$) is reached. Thus the hysteresis should disappear as instability is approached, as is observed experimentally: this can be seen particularly clearly in Fig. 2. Experimentally, δI is found to be different in sweep up and sweep down, indicating that α is in fact different in the PDR regions above and below the NDR region. This complicates the analysis without altering the qualitative conclusions.

An applied transverse magnetic field causes redistribution of the tunneling electron momentum and energy. In order to

conserve the momentum and energy in the tunneling process, the resonant peak voltage shifts to a higher value, the peak-current decreases, and the width of the resonance peak increases with increasing B . As a result, ΔI and β decrease with increasing magnetic field. Similarly, increasing sample temperature enhances the inelastic scattering through the barrier, increasing the valley current in $I(V)$ and broadening the resonant tunneling peak so as to reduce tunneling peak current. As a result, ΔI and β decrease with increasing sample temperature. Consequently, we expect the transverse magnetic field and sample temperature to have a similar effect on $I(U)$. Increasing magnetic field or sample temperature should both reduce the hysteresis and produce the transition between static and dynamic EFD formation. As can be seen in Figs. 1–4, we have demonstrated that a transverse magnetic field (B) or sample temperature can indeed induce such a transition. At low temperature ($T = 1.6$ K) and zero field, $I(U)$ exhibits static EFD formation. A large current hysteresis is observed in $I(U)$ when the applied bias is swept in the up- and down-directions. At high magnetic field ($10.5 \text{ T} < B < 12.5 \text{ T}$ and $T = 1.6$ K) or high temperature ($170 \text{ K} < T < 190 \text{ K}$ and $B = 0$), the hysteresis in $I(U)$ disappears and we observe the dynamic field domain formation, manifested in temporal current self-oscillation at a frequency of a few MHz, in a certain range of d.c. bias. Further increase of magnetic field or temperature produces an uniform electric field distribution.

In conclusion, we have observed the current self-oscillation in a doped GaAs/AlAs SL induced by both a transverse magnetic field and the sample temperature. The oscillations can be attributed to the EDF instabilities due to NDR. In particular, we find the following: (1) on increasing the strength of the magnetic field or the sample temperature at zero magnetic field, the negative differential $I(V)$ characteristic of a single barrier in a SL made up of N such barriers becomes flat (NDR increases). The current hysteresis, which is observed when the applied bias is swept in the up- and down-directions, decreases gradually. The hysteresis loop vanishes when the temperature or the strength of the magnetic field reached a certain value. (2) We verify the recent theory [26], which has shown that the transition is controlled by the magnitude of NDR. In particular, it shows that varying charge density, as well as varying transverse magnetic field and/or temperature, can all change the magnitude of NDR—although the microscopic mechanisms are quite different. This is an important conclusion as it clarifies the underlying physics for the transition from static to dynamic EFD formation in a SL structure.

Acknowledgements

The authors are especially grateful to Prof. M.D. Sturge for his many useful comments and critical reading of the

manuscript. The authors would like to thank Prof. P. Sheng, Prof. D.S. Jiang, Prof. Q. Niu, Dr W.K. Ge, and Dr Y.Q. Wang for valuable discussions. X.R.W., would like to thank the hospitality of the Center for Theoretical Science, Taiwan. The work is supported by the Research Grant Council, Hong Kong, China.

References

- [1] L.L. Chang, L. Esaki, R. Tsu, Appl. Phys. Lett. 24 (1974) 593.
- [2] L. Esaki, L.L. Chang, Phys. Rev. Lett. 33 (1974) 495.
- [3] F. Capasso, Physics of Quantum Electron Devices, Springer, New York, 1990.
- [4] F. Capasso, K. Mohammed, A.Y. Cho, Appl. Phys. Lett. 48 (1986) 478.
- [5] J.N. Schulman, J. Appl. Phys. 60 (1986) 3954.
- [6] T.B. Boyki, J.P. van der Wagt, J.S. Harris Jr., Phys. Rev. B 43 (1991) 4777.
- [7] T. Weil, B. Vinter, Appl. Phys. Lett. 50 (1987) 1281.
- [8] M.C. Payne, J. Phys. C 19 (1986) 1145.
- [9] B. Laikhtman, D. Miller, Phys. Rev. B 48 (1993) 5395.
- [10] F. Pregel, A. Wacker, E. Schöll, Phys. Rev. B 50 (1994) 1705.
- [11] L.L. Bonilla, J. Galan, J.A. Cuesta, F.C. Martfnez, J.M. Molera, Phys. Rev. B 50 (1994) 8644.
- [12] A. Wacker, M. Moscoso, M. Kindelan, L.L. Bonilla, Phys. Rev. B 55 (1997) 2466.
- [13] A. Wacker, A.P. Jauho, Phys. Rev. Lett. 80 (1998) 369.
- [14] H.T. Grahn (Ed.), Semiconductor Superlattices: Growth and Electronic Properties World Scientific, Singapore, 1995.
- [15] K.K. Choi, B.F. Levine, C.G. Bethea, J. Walker, R.J. Malik, Appl. Phys. Lett. 50 (1987) 1814.
- [16] K.K. Choi, B.F. Levine, N. Jarosik, J. Walker, R.J. Malik, Phys. Rev. B 38 (1988) 12 362.
- [17] Y. Zhang, Y. Li, D. Jiang, X. Yang, P. Zhang, Appl. Phys. Lett. 64 (1994) 3416.
- [18] S.H. Kwok, R. Merlin, H.T. Grahn, K. Ploog, Phys. Rev. B 50 (1994) 2007.
- [19] H.T. Grahn, R.J. Haug, W. Müller, K. Ploog, Phys. Rev. Lett. 67 (1991) 1618.
- [20] H.T. Grahn, J. Kastrup, K. Ploog, L.L. Bonilla, J. Galan, M. Kindelan, M. Moscoso, Jpn. J. Appl. Phys. 34 (1995) 4526.
- [21] J. Kastrup, R. Klann, H.T. Grahn, K. Ploog, L.L. Bonilla, J. Galan, M. Kindelan, M. Moscoso, R. Merlin, Phys. Rev. B 52 (1995) 13 761.
- [22] H. Mimura, M. Hosoda, N. Ohtani, K. Tominaga, K. Fujita, T. Watanabe, H.T. Grahn, K. Fujiwara, Phys. Rev. B 54 (1996) R2323.
- [23] M. Hosoda, H. Mimura, N. Ohtani, K. Tominaga, T. Watanabe, K. Fujiwara, H.T. Grahn, Appl. Phys. Lett. 69 (1996) 500.
- [24] S.H. Kwok, T.B. Norris, L.L. Bonilla, J. Galan, J.A. Cuesta, F.C. Martfnez, J.M. Molera, H.T. Grahn, K. Ploog, R. Merlin, Phys. Rev. B 51 (1995) 10 171.
- [25] Y. Zhang, J. Kastrup, R. Klann, K. Ploog, H.T. Grahn, Phys. Rev. Lett. 77 (1996) 3001.
- [26] X.R. Wang, Q. Niu, Phys. Rev. B 59 (1999) R12 755.